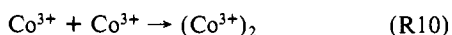
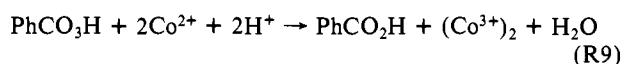
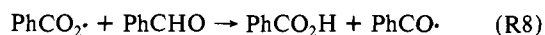
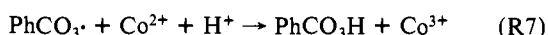
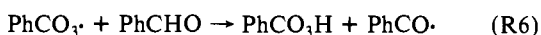
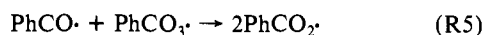
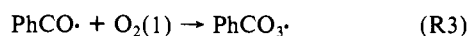
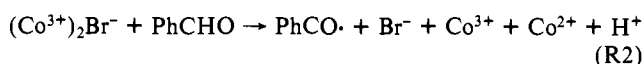
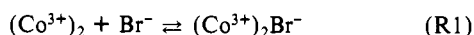


rate of oxygen consumption, which we view as associated with the exponentially increasing  $[\text{Co}^{3+}]$  (see below), exceeds the constant rate at which  $\text{O}_2$  is being supplied to the solution. When  $[\text{O}_2(1)] \approx \text{O}$ , stage II begins (the potential begins to fall) and  $\text{Co}^{3+}$  is rapidly converted back to  $[\text{Co}^{2+}]$ .

If  $[\text{O}_2(1)]$  is always appreciably less than saturation, then the rate of mass transfer of oxygen from the gas phase into the liquid determines the average rate of oxidation of PhCHO. The average rate of disappearance of PhCHO (measured by high-performance liquid chromatography) during a batch reaction is indeed zero order in  $[\text{PhCHO}]$ . Within a given oscillatory cycle,  $[\text{PhCHO}]$  shows a rapid decrease during stage II, suggesting that benzaldehyde reduces  $\text{Co}^{3+}$  in stage II.

Although oscillations did not occur without bromide ion under our conditions,  $[\text{Br}^-]$  (measured using a  $\text{Br}^-$ -selective electrode, Orion) was essentially constant during oscillations. In the Belousov-Zhabotinsky and other bromate-driven oscillators, changes in  $[\text{Br}^-]$  of several orders of magnitude are an essential feature of the mechanism.<sup>5</sup>

To account for these observations, we propose the following mechanism for the oxidation:



Although the radicals have been written here in the standard form, they may exist in solution complexed with Co ion, leading to unusual chemical behavior, e.g., (R5).

Initiation steps R1 and R2 use a  $\text{Co}^{3+}$  dimer,  $(\text{Co}^{3+})_2$ , to produce a benzoyl radical at a rate proportional to the product of  $[\text{PhCHO}]$ ,  $[\text{Br}^-]$ , and  $[(\text{Co}^{3+})_2]$ . During stage I, benzoyl radical is rapidly intercepted by oxygen in (R3) to form the perbenzoxy radical. (R6) continues the radical chain, while (R7) terminates it. (R3), (R6), and (R7) are well established.<sup>6,7</sup> The rapid oxidation of  $\text{Co}^{2+}$  by perbenzoic acid, (R9), then completes the autocatalytic generation of  $(\text{Co}^{3+})_2$ .<sup>8</sup>

It is only when oxygen becomes severely depleted that stage II begins, the benzoyl radical lifetime increases, and its concentration rises sharply. During stage II,  $(\text{Co}^{3+})_2$  is reduced by benzaldehyde through the intermediacy of benzoyl radicals in R4 + R8. The sequence (R5) followed by  $2 \times (\text{R8})$  provides an alternate fate for perbenzoxy radicals during stage II which does not generate more  $\text{Co}^{3+}$ .

(5) Noyes, R. M. *J. Am. Chem. Soc.* **1980**, *102*, 4644-4649.

(6) Sheldon, R. A.; Kochi, J. K. "Metal-Catalyzed Oxidations of Organic Compounds"; Academic Press: New York, 1981.

(7) Hendriks, C. F.; van Beek, H. C. A.; Heertjes, P. M. *Ind. Eng. Chem. Prod. Res. Dev.* **1978**, *17*, 260-264.

(8) The rate of oxidation of  $\text{Co}^{2+}$  by *m*-chloroperbenzoic acid is reported to be second order in  $[\text{Co}^{2+}]$  and first order in peracid.<sup>3</sup> Addition of perbenzoic acid ( $[\text{PhCO}_3\text{H}]/[\text{total Co}] = 0.05$ ) during the middle of stage I results in a rapid ( $< 1$  s) increase in both potential and  $[\text{Co}^{3+}]$ . This indicates that (R9) is rapid and that perbenzoic acid does not accumulate from cycle to cycle. Possible variations involving thermal rearrangements<sup>3</sup> of  $(\text{Co}^{3+})_2$ , ligand variation on Co, and other Co-containing oligomers have not been considered here.

The rate equations<sup>9</sup> for (R1)-(R11) were integrated using a Gear algorithm,<sup>10</sup> with the results shown in Figure 2. The qualitative agreement with the experimentally measured  $[\text{Co}^{3+}]$  and  $[\text{O}_2(1)]$  oscillations of Figure 1 is encouraging.

In conclusion, we propose that the  $\text{Co}^{2+}/\text{Br}^-$ -catalyzed  $\text{O}_2$  oxidation of benzaldehyde differs from oxyhalogen-driven oscillators, in that an organic radical is one of the oscillatory, phase-determining intermediates. An essential feature of the oscillations is a periodic depletion of dissolved oxygen, allowing for the alternative pathway of  $\text{Co}^{3+}$  oxidation of benzoyl radicals.

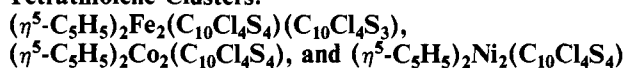
**Acknowledgment.** We thank A. P. Berry for excellent experimental assistance.

**Registry No.** Benzaldehyde, 100-52-7; cobaltous acetate, 71-48-7; sodium bromide, 7647-15-6.

(9) The simulation is for a batch mode, except for the flow of  $\text{O}_2$ . Rate constants used were  $(k_1 k_2)/k_{-1} = 2.5 \times 10^{-1} \text{ M}^{-2} \text{ s}^{-1}$ ,  $k_{-1} \gg k_2$ ,  $k_3 = 1 \times 10^8 \text{ M}^{-1} \text{ s}^{-1}$ ,  $k_4 = 2 \times 10^4 \text{ M}^{-1} \text{ s}^{-1}$ ,  $k_5 = 2 \times 10^8 \text{ M}^{-1} \text{ s}^{-1}$ ,  $k_6 = 1 \times 10^4 \text{ M}^{-1} \text{ s}^{-1}$ ,  $k_7 = 8 \times 10^4 \text{ M}^{-1} \text{ s}^{-1}$ ,  $k_8 = 1 \times 10^5 \text{ M}^{-1} \text{ s}^{-1}$ ,  $k_9 = 1 \times 10^9 \text{ M}^{-2} \text{ s}^{-1}$ ,  $k_{10} = 1 \times 10^6 \text{ M}^{-1} \text{ s}^{-1}$ ,  $k_{-11} = 1 \times 10^{-2} \text{ s}^{-1}$ , and  $k_{11}/k_{-11} = 6 \times 10^{-3} \text{ M (atm O}_2\text{)}^{-1}$ . Initial concentrations were  $[\text{PhCHO}] = 750 \text{ mM}$ ,  $[\text{total Co}] = 20 \text{ mM}$ ,  $[\text{Br}^-] = 10 \text{ mM}$ .  $\text{O}_2(\text{g})$  pressure was held constant at 580 torr, and  $[\text{H}^+]$  is incorporated in the rate constants.

(10) Stabler, R. N.; Chesick, J. *Int. J. Chem. Kinet.* **1978**, *10*, 461-469.

### Syntheses and Structures of a Novel Series of Tetrathiolene Clusters:



Boon K. Teo,\* V. Bakirtzis, and P. A. Snyder-Robinson

Bell Laboratories  
Murray Hill, New Jersey 07974

Received February 22, 1983

Recently we reported the synthesis and characterization of a novel series of metal tetrathiolene complexes containing 1, 2, 2, 3, and 4 metals and corresponding to 2, 4, 6, 8, and 12 electron-donating ligand systems, respectively.<sup>1</sup> In an attempt to prepare the "six-electron" systems  $(\eta^5\text{-C}_5\text{H}_5)_2\text{M}_2(\text{C}_{10}\text{Cl}_4\text{S}_4)$  where M = Fe, Co, and Ni, which span the metal-metal bond orders of 2 (Fe=Fe), 1 (Co-Co), and 0 (Ni-Ni), the ligand  $\text{C}_{10}\text{Cl}_4\text{S}_4$  (TCTTN)<sup>2</sup> was reacted with  $(\eta^5\text{-C}_5\text{H}_5)_2\text{Fe}_2(\text{CO})_4$ ,  $(\eta^5\text{-C}_5\text{H}_5)\text{-Co}(\text{CO})_2$ , and  $(\eta^5\text{-C}_5\text{H}_5)_2\text{Ni}_2(\text{CO})_2$ , respectively. To our surprise, the iron complex reacts differently from the cobalt and the nickel analogues. Instead of forming the anticipated Fe=Fe bond it yielded  $(\eta^5\text{-C}_5\text{H}_5)_2\text{Fe}_2(\text{C}_{10}\text{Cl}_4\text{S}_4)(\text{C}_{10}\text{Cl}_4\text{S}_4)$  via a *facile desulfurization* reaction of one of the TCTTN ligands under very mild conditions. The corresponding cobalt and nickel reactions gave rise to  $(\eta^5\text{-C}_5\text{H}_5)_2\text{Co}_2(\text{C}_{10}\text{Cl}_4\text{S}_4)$  with a Co-Co single bond and  $(\eta^5\text{-C}_5\text{H}_5)_2\text{Ni}_2(\text{C}_{10}\text{Cl}_4\text{S}_4)$  with no Ni-Ni bond.

The title compounds  $(\eta^5\text{-C}_5\text{H}_5)_2\text{Fe}_2(\text{C}_{10}\text{Cl}_4\text{S}_4)(\text{C}_{10}\text{Cl}_4\text{S}_4)$  (1),  $(\eta^5\text{-C}_5\text{H}_5)_2\text{Co}_2(\text{C}_{10}\text{Cl}_4\text{S}_4)$  (2), and  $(\eta^5\text{-C}_5\text{H}_5)_2\text{Ni}_2(\text{C}_{10}\text{Cl}_4\text{S}_4)$  (3) were prepared by reacting  $(\eta^5\text{-C}_5\text{H}_5)_2\text{Fe}_2(\text{CO})_4$ ,  $(\eta^5\text{-C}_5\text{H}_5)\text{-Co}(\text{CO})_2$ , and  $(\eta^5\text{-C}_5\text{H}_5)_2\text{Ni}_2(\text{CO})_2$ , respectively, with  $\text{C}_{10}\text{Cl}_4\text{S}_4$  (TCTTN)<sup>2</sup> in a metal:TCTTN = 2:1 molar ratio in refluxing benzene for ca 12-24 h. The dark brown or dark red precipitates thus formed were filtered, washed with benzene and acetonitrile, and vacuum dried. The yields were 40, 65, and 77% for 1, 2, and 3, respectively. The crude products were recrystallized from either  $\text{CHCl}_3/\text{CH}_3\text{CN}$  or  $\text{CHCl}_3/\text{toluene}$ . All three compounds gave satisfactory elemental analyses.

The molecular architecture of the title compounds are depicted in Figures 1-3. Crystallographic details are summarized in the supplementary material.

(1) Teo, B. K.; Snyder-Robinson, P. A. *Inorg. Chem.* **1981**, *20*, 4235 and references cited therein.

(2) Klingsberg, E. *Tetrahedron*, **1972**, *28*, 963.

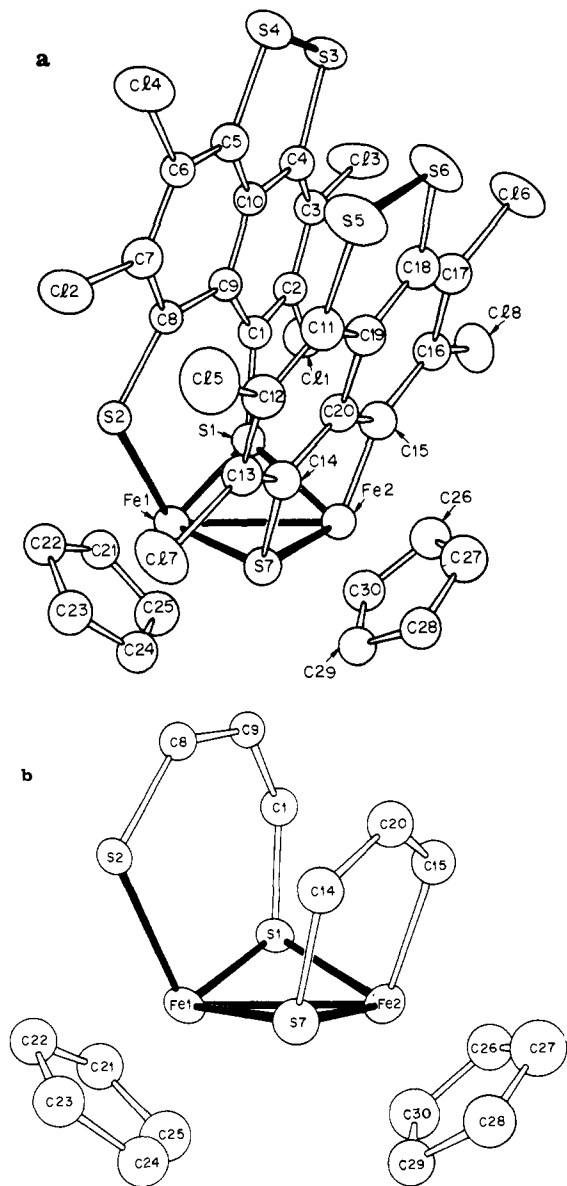


**Figure 1.** Structure (ORTEP, 50% probability ellipsoids) of  $(\eta^5\text{-C}_5\text{H}_5)_2\text{Fe}_2(\text{C}_{10}\text{Cl}_4\text{S}_4)(\text{C}_{10}\text{Cl}_4\text{S}_3)$  (**1**): (a) general view; (b) core structure. Distances in Å, angles in deg: Fe1–Fe2, 2.649 (4); Fe1–S1, 2.160 (5); Fe1–S2, 2.238 (5); Fe1–S7, 2.242 (6); Fe2–S1, 2.226 (6); Fe2–S7, 2.188 (5); Fe2–C15, 2.013 (19); S1...S2, 3.244 (7); S3–S4, 2.077 (8); S5–S6, 2.086 (8); S1–C1, 1.782 (18); S2–C8, 1.721 (18); S7–C14, 1.760 (18); Fe1–C(C<sub>5</sub>H<sub>5</sub>), 2.133 (av); Fe2–C(C<sub>5</sub>H<sub>5</sub>), 2.107 (av); Fe1–S1–Fe2, 74.28 (17); Fe1–S7–Fe2, 73.41 (17).

The structure of **1** can be described as two  $\text{Fe}(\eta^5\text{-C}_5\text{H}_5)$  units bridged by two nearly parallel ligands,  $\text{C}_{10}\text{Cl}_4\text{S}_4$  (hereafter referred to as ligand 1) and  $\text{C}_{10}\text{Cl}_4\text{S}_3$  (hereafter referred to as ligand 2). The observed Fe–Fe distance of 2.649 (4) Å is consistent with a single Fe–Fe bond.<sup>3–8</sup> The two iron atoms are bridged by two sulfur atoms, S1 from ligand 1 and S7 from ligand 2. While Fe1 has S2 from ligand 1 as a terminal ligand, Fe2 has C15 from ligand 2 as the terminal ligand. Each iron thus adopts a pseudo-octahedral coordination.

(3) For example, the iron–iron distances in  $[(\eta^5\text{-C}_5\text{H}_5)_2\text{Fe}_2(\text{CO})_2(\text{PPh}_2)_2]^n$  where  $n = 0, +1,$  and  $+2$  are 3.498 (4), 3.14 (2), and 2.764 (4) Å, corresponding to bond order of 0,  $1/2,$  and 1, respectively.<sup>4</sup> The Fe=Fe double bond in  $\text{Fe}_2(\text{CO})_4(\text{C}_2\text{R}_2\text{S}_2)$  is 2.225 (3) Å.<sup>5</sup>

(4) Sinclair, J. D.; Dahl, L. F., private communication.

(5) Schmitt, H.-J.; Ziegler, M. L. *Z. Naturforsch. B* **1973**, *28*, 508.

(6) The Fe–Fe single-bond distances in  $\text{Fe}_2(\text{CO})_6(\text{SEt})_2^7$  and  $\text{Fe}_4(\text{CO})_{12}(\text{C}_2\text{S}_4)^8$  are 2.537 (10) and 2.486 (2) Å, respectively.

(7) Dahl, L. F.; Wei, C. H. *Inorg. Chem.* **1963**, *2*, 328.

(8) Broadhurst, P. V.; Johnson, B. F. G.; Lewis, J.; Raithby, P. R. *J. Chem. Soc., Chem. Commun.* **1982**, 140.

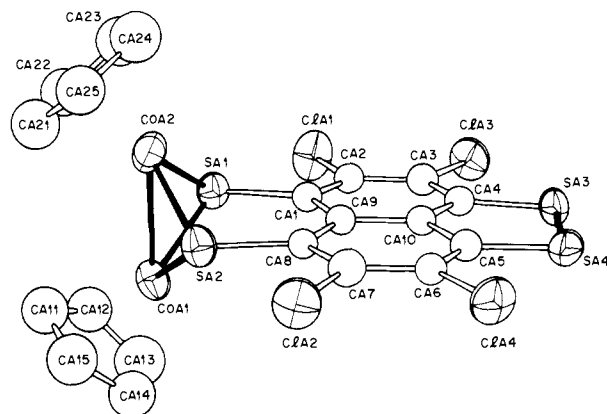


**Figure 2.** Structure (ORTEP, 50% probability ellipsoids) of molecule A of  $(\eta^5\text{-C}_5\text{H}_5)_2\text{Co}_2(\text{C}_{10}\text{Cl}_4\text{S}_4)$  (**2**). Distances in Å, angles in deg, for molecule A and B: Co1–Co2, 2.415 (3), 2.434 (3); Co1–S1, 2.175 (4), 2.182 (4); Co1–S2, 2.177 (4), 2.169 (4); Co2–S1, 2.160 (4), 2.181 (4); Co2–S2, 2.173 (4), 2.166 (4); S1...S2, 3.020 (5), 3.035 (5); S3–S4, 2.076 (5), 2.074 (6); Co1–C(C<sub>5</sub>H<sub>5</sub>), 2.063 (av), 2.067 (av); Co2–C(C<sub>5</sub>H<sub>5</sub>), 2.059 (av), 2.075 (av); Co1–S1–Co2, 67.71 (13), 67.82 (13); Co1–S2–Co2, 67.45 (13), 68.33 (14).

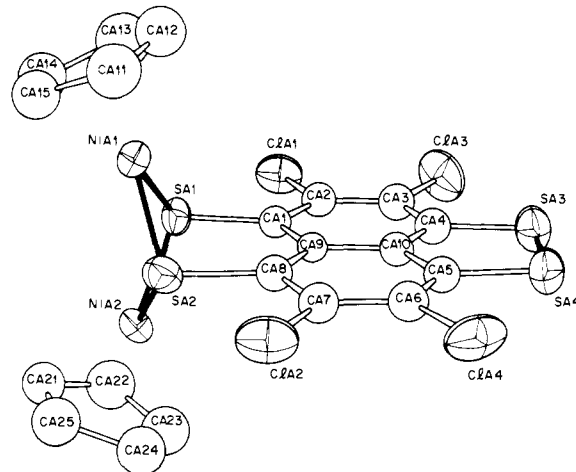


**Figure 3.** Structure (ORTEP, 50% probability ellipsoids) of molecule A of  $(\eta^5\text{-C}_5\text{H}_5)_2\text{Ni}_2(\text{C}_{10}\text{Cl}_4\text{S}_4)$  (**3**). Distances in Å, angles in deg, for molecule A and B: Ni1...Ni2, 2.951 (3), 2.809 (3); Ni1–S1, 2.163 (5), 2.164 (4); Ni1–S2, 2.173 (4), 2.181 (4); Ni2–S1, 2.168 (4), 2.162 (4); Ni2–S2, 2.158 (5), 2.170 (4); S1...S2, 2.936 (6), 2.974 (5); S3–S4, 2.053 (8), 2.069 (7); Ni1–C(C<sub>5</sub>H<sub>5</sub>), 2.110 (av), 2.102 (av); Ni2–C(C<sub>5</sub>H<sub>5</sub>), 2.114 (av), 2.103 (av); Ni1–S1–Ni2, 85.89 (16), 80.99 (15); Ni1–S2–Ni2, 85.90 (16), 80.41 (15).

The most important chemical and structural feature of **1** is the loss of one sulfur atom from one of the TCTTN ligands and the formation of an iron–carbon(aryl)  $\sigma$  bond (Fe2–C15). As shown in Figure 1, the Fe2–C15 distance of 2.013 (19) Å corresponds to a single covalent bond.<sup>9–11</sup> The core structure of **1** (cf. Figure 1b) can be described as three fused heterocyclic rings with six ( $\text{FeS}_2\text{C}_3$ ), four ( $\text{Fe}_2\text{S}_2$ ), and five ( $\text{FeSC}_3$ ) members. The Fe–S distances within the six- and the five-membered chelate rings (Fe1–S1 of 2.160 (5) and Fe2–S7 of 2.188 (5) Å) are significantly shorter than those between rings (Fe1–S7 of 2.242 (6) and Fe2–S1 of 2.226 (6) Å). Within the six-membered chelate ring, the terminal Fe1–S2 distance of 2.238 (5) Å is significantly longer than the bridging Fe1–S1 distance of 2.160 (5) Å. (Note that the shorter metal–sulfur distances are comparable to the average value of 2.173 (4) and 2.167 (4) Å in **2** and **3**, respectively.) It

(9) For example, the Fe–C(aryl)  $\sigma$  bonds in  $[\text{Fe}(\text{C}_{22}\text{H}_{22}\text{N}_4)\text{C}_6\text{H}_5]^{10}$  and in  $[\text{Fe}_2(\text{CO})_8\text{C}_6\text{F}_4]^{11}$  were found to be 1.933 (3) and 2.022 (3) Å, respectively.

(10) Goedken, V. L.; Peng, S. M.; Park, Y. A. *J. Am. Chem. Soc.* **1974**, *96*, 284.

(11) Bennett, M. J.; Graham, W. A. G.; Stewart, R. P., Jr.; Tuggle, R. M. *Inorg. Chem.* **1973**, *12*, 2944.

is also of interest to note that the long Fe1-S2 distance of 2.238 (5) Å is accompanied by a short S2-C8 distance of 1.721 (18) Å, in contrast to the corresponding values of 2.160 (5) (Fe1-S1) and 1.782 (18) Å (S1-C1). The two intact S-S bond lengths in **1** are 2.077 (8) Å (S3-S4) and 2.086 (8) Å (S5-S6).

The structure of **2** (Figure 2) or **3** (Figure 3) can be described as two  $M(\eta^5-C_5H_5)$  moieties bridged by two sulfur atoms (S1 and S2) (in a butterfly-like arrangement) from one end of the TCTTN ligand via oxidative addition, leaving the other S3-S4 bond intact at ca. 2.07 Å. There is a single Co-Co bond of 2.415 (3) (molecule A) or 2.434 (3) (molecule B) in **2** but nonbonding Ni...Ni contacts at 2.951 (3) (molecule A) or 2.809 (3) Å (molecule B) in **3**, in accord with the noble gas rule. The average Co-Co distance of 2.425 Å in **2** is among the shortest single cobalt-cobalt bonds known (e.g.,  $(\eta^5-C_5H_5)_2Co_2(PPh_2)_2$ ,<sup>12</sup> 2.56 (1) Å;  $Co_2(CO)_6(C_2(t-Bu)_2)$ ,<sup>13</sup> 2.463 (1) Å). The average Ni...Ni distance of 2.880 Å is among the shortest nonbonding nickel...nickel distances known (e.g.,  $(\eta^5-C_5H_5)_2Ni_2(PPh_2)_2$ ,<sup>12</sup> 3.36 (1) Å). In fact, it is even 0.26 Å shorter than the metal-metal distance of 3.14 Å in  $[(\eta^5-C_5H_5)_2Fe_2(CO)_2(PPh_2)_2]^+$  with a formal bond order of  $1/2$ .<sup>3</sup> The soft Ni...Ni interaction is probably responsible for the 0.14 Å difference in the Ni...Ni distance between the two independent molecules in the unit cell. The stereochemical contrast between **2** and **3** on the one hand and  $(\eta^5-C_5H_5)_2M_2(PPh_2)_2$  where M = Co and Ni on the other is rather interesting.

It is interesting to compare the dihedral angle (angle between the normals) between the two  $MS_2$  planes within the butterfly-like  $M_2S_2$  fragment in **2** and **3**. The values are 78.6° and 77.2° for **2** and 44.1° and 54.5° for **3** for molecules A and B, respectively. Apparently, the addition of two electrons to the metal-metal antibonding orbital (presumed to be the lowest unoccupied molecular orbital)<sup>14</sup> in the dicobalt species to form the dinickel cluster is responsible for the opening of the  $M_2S_2$  fragment and the drastic change in the dihedral angle of ca. 30°. Furthermore, while the dihedral angle formed by the  $C_3S_2$  plane and the  $MS_2$  plane in all the structurally characterized metal tetrathiolene complexes<sup>1</sup> generally fall in the range of 38.9-52.8°, the values are 50.4-51.8° in **2** and 62.6-68.0° in **3**. We note that the observed Ni...Ni distance of 2.880 Å in **3** is not far from the limiting distance of 3.184 (molecule A) or 3.159 Å (molecule B) at the extreme dihedral angle of 90° between the  $C_3S_2$  and  $MS_2$  planes (or 0° between the two  $MS_2$  planes).

It is conceivable that the sought-after Fe=Fe double bond, presumably formed in the early stage(s) of the reaction of  $(\eta^5-C_5H_5)_2Fe_2(CO)_4$  with TCTTN, is so reactive that it further reacts with TCTTN with the unexpected elimination of one sulfur to form **1**.<sup>15,16</sup> At least one other major product in the filtrate of the reaction has been identified by HPLC.<sup>17</sup> Characterization (in progress) of this or other reaction products will eventually provide evidence for the fate of the "lost" sulfur atom as well as shed light on the desulfurization process. Nevertheless, the present study represents a new example of desulfurization of aryl disulfides (and the first example for the tetrathiolene ligands) under very mild conditions (at atmospheric pressure, low temperature, and in the absence of hydrogen).<sup>18,19</sup>

(12) Coleman, J. M.; Dahl, L. F. *J. Am. Chem. Soc.* **1967**, *89*, 542.  
(13) Cotton, F. A.; Jamerson, J. D.; Stults, B. R. *J. Am. Chem. Soc.* **1976**, *98*, 1774.

(14) (a) Teo, B. K.; Hall, M. B.; Fenske, R. F.; Dahl, L. F. *Inorg. Chem.* **1975**, *14*, 3103. (b) *J. Organomet. Chem.* **1974**, *70*, 413.

(15) The "reverse" reaction, viz., the addition of sulfurs to a ligand such as  $CS_2$  via a metal complex, is also possible (see, for example, ref 16).

(16) Coucouvanis, D.; Draganjac, M. *J. Am. Chem. Soc.* **1982**, *104*, 6820.

(17) Teo, B. K.; Bakirtzis, V., work in progress.

(18) For other stoichiometric desulfurization reactions, see the work of Alper.<sup>20</sup> Kaesz,<sup>21</sup> Gilman,<sup>22</sup> Weiss,<sup>23</sup> Dilworth,<sup>24</sup> Eisch,<sup>25</sup> and others.

(19) It is interesting to note that most industrial processes for the removal of organic sulfur from petroleum or coal or as a pollutant involves hydrodesulfurization at high temperature (350-450 °C) and high pressure (33-165 atm) in the presence of catalysts such as presulfided cobalt-molybdena or nickel-tungsten supported on alumina.<sup>26-36</sup>

(20) (a) Alper, H.; Paik, H. N. *J. Org. Chem.* **1977**, *42*, 3522. (b) Alper, H.; Prince, T. L. *Angew. Chem., Int. Ed. Engl.* **1980**, *19*, 315. (c) Alper, H.; Blais, C. *Fuel* **1980**, *59*, 670.

**Supplementary Material Available:** Listing of experimental data for **1**, **2**, and **3** (2 pages). Ordering information is given on any current masthead page.

(21) (a) Kaesz, H. D.; King, R. B.; Manuel, T. A.; Nichols, L. D.; Stone, F. G. A. *J. Am. Chem. Soc.* **1960**, *82*, 4749. (b) Porter, C. R.; Kaesz, H. D.; Leto, J. L.; Giordano, T. J.; Haas, W. R.; Johnson, E.; Berry, W. H., Jr. *Coal Process. Technol.* **1981**, *7*, 135.

(22) (a) Gilman, H.; Esmay, D. L. *J. Am. Chem. Soc.* **1953**, *75*, 2947. (b) Gilman, H.; Dietrich, J. J. *J. Org. Chem.* **1957**, *22*, 850. (c) Gilman, H.; Dietrich, J. J. *J. Am. Chem. Soc.* **1958**, *80*, 380.

(23) Weiss, L. H. *Proc. Intersoc. Energy Convers. Eng. Conf.* **1976**, *11* (1), 309.

(24) Blower, P. J.; Dilworth, J. R.; Hutchinson, J. P.; Zubieta, J. A. *Inorg. Chim. Acta* **1982**, *65*, L225.

(25) (a) Eisch, J. J.; Im, K. R. *J. Organomet. Chem.* **1977**, *139*, C51; (b) *Adv. Chem. Ser.* **1979**, *173*, 195. (c) Eisch, J. J.; Im, K. R.; Hallenbeck, L. E. *Prepr. Div. Pet. Chem., Am. Chem. Soc.* **1980**, *25*, 224.

(26) Weisser, O.; Landa, S. "Sulphide Catalysis, Their Properties and Applications"; Pergamon: Elmsford, NY, 1973.

(27) Gates, B. C.; Katzer, J. R.; Schuit, G. C. A. "Chemistry of Catalytic Processes"; McGraw-Hill: New York, 1979; Chapter 5.

(28) Mitchell, P. C. H. "Catalysis", The Chemical Society: London, 1977, Vol. 1, A Specialist Periodical Report, Chapter 6.

(29) Massoth, F. E. *Adv. Catal.* **1978**, *27*, 265.

(30) Donati, E. E. *Adv. Catal.* **1956**, *8*, 39.

(31) Voorhoeve, R. J. H.; Stuiver, J. C. M. *J. Catal.* **1971**, *23*, 228.

(32) Rollman, L. D. *J. Catal.* **1977**, *46*, 243.

(33) Pecoraro, T. A.; Chianelli, R. R. *J. Catal.* **1981**, *67*, 430.

(34) Givens, E. N.; Venuto, P. B. *Prepr., Div. Petrol. Chem., Am. Chem. Soc.* **1970**, *15* (4), A183.

(35) Schuit, G. C. A.; Gates, B. C. *AIChE J.* **1973**, *19*, 417.

(36) Bartsch, R.; Tanielian, C. *J. Catal.* **1974**, *35*, 353.

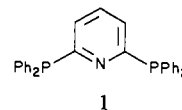
## Phosphine Ligands for the Construction of Polynuclear Complexes. 2. 2,6-Bis(diphenylphosphino)pyridine Complexes of Palladium(II) and Rhodium(I)

Fred E. Wood, Marilyn M. Olmstead, and Alan L. Balch\*

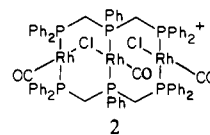
Department of Chemistry, University of California  
Davis, California 95616

Received January 13, 1983

As part of our studies<sup>1,2</sup> exploring the use of polyfunctional phosphine ligands for the construction of multinuclear transition-metal complexes, we have examined the coordination behavior of 2,6-bis(diphenylphosphino)pyridine (**1**) ( $(Ph_2P)_2py$ ).<sup>3</sup> In this



paper we compare and contrast the binding of two  $d^8$  metal ions, Pd(II) and Rh(I) with **1** and the related triphosphine bis(diphenylmethyl)phenylphosphine (dpmp). The latter forms a simple, chelated complex,  $(dpmp)PdCl_2$ , with palladium and a remarkable trinuclear complex, **2**, with rhodium.



The ligand  $(Ph_2P)_2py$  is closely related to 2-(diphenylphosphino)pyridine ( $Ph_2Ppy$ ), which has been useful in constructing binuclear, particularly heterobinuclear, complexes.<sup>3</sup> Because of the location of the pyridine ring,  $(Ph_2P)_2py$  is con-

(1) Guimerans, R. R.; Olmstead, M. M.; Balch, A. L. *J. Am. Chem. Soc.* **1983**, *105*, 1677-1679.

(2) (a) Farr, J. P.; Olmstead, M. M.; Balch, A. L. *J. Am. Chem. Soc.* **1980**, *101*, 6654-6656. (b) Maisonnat, A.; Farr, J. P.; Olmstead, M. M.; Hunt, C. T.; Balch, A. L. *Inorg. Chem.* **1982**, *21*, 3961-3967. (c) Farr, J. P.; Olmstead, M. M.; Wood, F.; Balch, A. L. *J. Am. Chem. Soc.* **1983**, *105*, 792-798.

(3) Newkome, G. R.; Hager, D. C. *J. Org. Chem.* **1978**, *43*, 947-949.